Proceedings of the ASME 2023
ICE Forward Conference
ICEF2023
October 8-11, 2023, Pittsburgh, Pennsylvania

ICEF2023-109875

UNDERSTANDING DIESEL-PILOT ASSISTED METHANE COMBUSTION IN A COMPRESSION IGNITION ENGINE

Amanda Sirna[1,2], Amir Hassan[1], Rodrigo Ristow Hadlich[1,2], Jason Loprete[1,2], Juan Pablo Trelles[3], Noah Van Dam[3], J. Hunter Mack[3], Dimitris Assanis[1,2,4,*]
[1]Stony Brook University, Stony Brook, NY
[2]Advanced Energy Research and Technology Center, Stony Brook, NY
[3]University of Massachusetts Lowell, Lowell, MA
[4]Institute for Advanced Computational Science, Stony Brook, NY

ABSTRACT

Developing a sustainable alternative to diesel and gasoline is critical to mitigating climate change effects. Methane, the primary component of natural gas, presents itself as a successor to petroleum-based fuels. Compared to other hydrocarbons, methane (CH_4) has the highest hydrogen to carbon ratio which means when combusted in an engine, fewer carbon-based emissions occur. Natural gas currently has an extensive distribution infrastructure. This makes it a realistic intermediary option as a fuel source until the zero carbon alternatives are understood. This work explores combustion of methane in a single cylinder compression ignition (CI) research engine. A small amount of diesel was used to promote ignition of the methane charge. An exploration of equivalence ratios and injection timings was conducted to seek stable operation and maximum brake torque (MBT). Trends of engine performance metrics, a heat release analysis, and an emission characterization are presented in this manuscript. Performance of methane with diesel pilot injection with blend ratios between 47-51% methane by energy content and 88-90% by volume are compared to a baseline single injection diesel case and a split injection (pilot and main) diesel case. The purpose of the diesel pilot in the methane case is to function as a "spark" for the methane, due to methane's longer ignition delay time. Key findings include that a dual fuel (diesel pilot + methane), dual injection strategy with a pilot injection event 5 degrees before top dead center (bTDC) maintained the most favorable balance between combustion performance and engine-out emissions. The implications of this study will help to better understand optimal strategies for maximizing the usefulness of methane as a primary fuel source in future dual fuel engines.

Keywords: Diesel; Pilot Injection; Methane; Dual Fuel Combustion; Compression Ignition Engine

NOMENCLATURE

Greek Letters:

ϕ	fuel-air equivalence ratio
$\eta_{f,ig}$	gross indicated fuel conversion efficiency

Abbreviations:

ATDC	after top dead center
BTDC	before top dead center
CAD	crank angle degree
CH_4	methane
CI	compression ignition
CNG	compressed natural gas
CO	carbon monoxide
CO_2	carbon dioxide
$IMEP_{gross}$	gross indicated mean effective pressure
LNG	liquified natural gas
MBT	maximum brake torque
N_2	nitrogen
NO_x	nitrogen oxide
O_2	oxygen
PM	particulate matter
RPM	revolutions per minute
SLPM	standard liters per minute
SOC	start of combustion
SOI	start of injection
TDC	top dead center
THC	total hydrocarbons

*Corresponding Author: dimitris.assanis@stonybrook.edu

1. INTRODUCTION

The global push to reduce harmful emissions is a multi-faceted and complex problem. In the United States, the transportation sector produced 27% of the country's total gross greenhouse gas emissions in 2020 [1]. Of that, medium and heavy-duty vehicles represent 26% of the previous figure, or about 7% of all emissions [1]. These figures do not include other combustion applications such as marine and aviation which also use petroleum-based fuels. Due to government regulations as well as growing public knowledge of climate change, alternative fuels have seen a rise in popularity. Research has reflected this shift, now looking into alternative fuels such as natural gas as well as alternative combustion modes such as dual-fuel combustion to help meet these new government regulations.

1.1 Natural Gas Usage

Today, many heavy-duty vehicles such as trucks and buses use natural gas enabled powertrains. Natural gas is also actively being researched for use in the electricity generation sector, where burning natural gas instead of coal or petroleum-based products has seen a reduction in carbon monoxide (CO), carbon dioxide (CO_2), and total hydrocarbon (THC) emissions [2]. Methane (CH_4) is the primary component of natural gas, making up to 85-95% of its chemical composition by volume [3,4]. This coupled with methane's high hydrogen to carbon ratio make it an attractive alternative fuel and a good surrogate fuel for research purposes. Natural gas can be stored and transported in two ways: compressed gas (CNG) and liquified (LNG) forms. The energy density of natural gas can be increased when stored in liquid state, which provides an attractive solution to using natural gas for longer distance travel [5]. This liquified state also has the benefit of taking advantage of a mature distribution network that is equipped to handle the transportation and refueling of liquids. When analyzing the greenhouse gas emissions of heavy-duty vehicles fueled with natural gas, it was found that natural gas can provide a moderate reduction in emissions when compared to diesel, with minimal difference in performance between CNG to LNG [6]. The potential benefits natural gas poses prove it is worth investigating its performance as a main fuel source.

1.2 Dual Fuel Combustion

Today's natural gas vehicles come in three forms: dedicated vehicles that only use natural gas, bi-fuel vehicles which may operate on either natural gas or gasoline/diesel, and dual fuel. Dual fuel vehicles are unique, as they use a mixture of two different reactivity fuels such as diesel and natural gas for operation. Their combustion process is the focus of this study. Dual fuel combustion typically requires the direct injection of a small amount of diesel into the cylinder to function as the ignition method for pre-mixed port injected methane and air [7]. This fueling and combustion strategy exploits the high reactivity of diesel fuel, which when injected close to top dead center (TDC), will auto-ignite [8]. The auto-ignition of diesel creates a flame which can propagate throughout the chamber and ignite the much less reactive gaseous methane-air blend. The pilot diesel ignition is needed to mitigate the longer ignition delay time and higher heat capacity properties of natural gas [9,10]. There are some concerns with this methodology. At low engine loads, flame extinction is a concern in lean regions of the fuel charge. At high loads, a practical knock limit exists. The presence of the diesel pilot will help alleviate some of these issues, which otherwise would be apparent when igniting natural gas in compression ignition (CI) engines. The amount of fuel required for the diesel pilot injection is small. It should be noted that if too little fuel is injected, misfire or incomplete combustion events may occur [8] and hence future experimental studies to investigate these phenomena have been recommended.

In past efforts, conversions of existing diesel compression ignition engines have been attempted. Shatrov et al. demonstrated through a new engine control unit, a two-stage gaseous fuel feed system, and a smaller diesel direct injection system could reduce CO_2 and NO_x emissions. One issue found was the reduction of IMEP values at low engine speeds which was partially attributed to the natural gas filling gaps between the cylinder head and the liner causing incomplete combustion [11]. This filling of the gaps is likely due to low turbulence at low speeds. Another challenge explained by Weaver and Turner is the loss of premixed air and natural gas through the exhaust valve due to prolonged valve overlap, increasing hydrocarbon emissions. In direct injected diesel engines, this scavenging effect is desired to maximize power output. Since the natural gas enters the cylinder via the intake port, the advantage of valve overlap quickly became a disadvantage [12]. This is supported by Taniguchi et al., who found that some retrofits would not meet the emissions standards set by certain governments [13]. As Caris and Nelson showed, a compression ratio between 14:1 and 18:1 was optimal for efficiency [14]. Raine et al. converted a 6.4-liter diesel bus engine for dual fuel use at a compression ratio of 15:1. At the time of writing, the bus traveled 58,000 kilometers, provided similar output with less noise, albeit at reduced throttle response, and achieved "virtually equal efficiencies" compared to its original configuration [15]. Thermo Power Corporation as well as Liu and Dumitrescu successfully showed methodologies to upgrade existing diesel engines to spark ignition and natural gas [16,17].

Manufacturers may solve the existing problems of upfitting current diesel engines in future natural gas variants through reductions in the tolerances between components, use of improved materials better suited for natural gas engines, modifying valve timing, using timed port fuel injection for the gaseous fuel, and prechamber ignition [12]. Retrofits of existing diesel powertrains to natural gas are an imperfect solution. However, the return on investment of extending the useful service life of the engine may incentivize their conversion [18].

1.3 Natural Gas as a Decarbonization Solution for CI

The largest impact of using natural gas instead of diesel as the main energy source in CI engines is the ability to reduce engine out emissions. Previous literature found less CO_2, nitrogen oxides (NO_x), and particulate matter (PM) [19]. Other studies found that carbon monoxide (CO) increased with methane when compared to diesel alone [20-22]. Through the

manipulation of injection timing and strategy, an optimum operating point can be located. It was found that a split injection method, with a 15% diesel charge by mass injected at 24 crank angle degrees (CAD) before top dead center and the remaining methane added at 8 degrees before TDC exhibited the best balance between performance and emissions [20]. To further enhance the reduction in emissions, natural gas and diesel can be swapped with their renewable counterparts, effectively creating a carbon neutral fuel mixture [23,24]. Renewable natural gas can be sourced from the off gas of the decomposition of organic matter [23]. The possibility of using a carbon-free alternative fuels to replace natural gas such as hydrogen, ammonia or blends thereof that match the flame speeds of natural gas is also a strong possibility [25, 26]. Ongoing work by Ran et al. [27] and Ristow Hadlich et al. [29, 30] are looking at the performance evaluation of naphthenic rich biofuels derived from the catalytic fast pyrolysis with hydrotreating pathway to replace fossil diesel in a compression ignition engine. Other approaches to enable dual fuel combustion with methane also include the use of additives, such as hydrogen peroxide by Hammond et al. [30].

In this experiment, a single diesel pilot will be used to ignite a primary methane fuel charge in a single cylinder compression ignition research engine. Since methane is the main component of natural gas, it will serve to be a reasonable trend wise-accurate representation of a practical natural gas dual fuel engine application. Further, Kakaee et al. [31] have previously investigated the effect of natural gas composition on natural gas fueled vehicle performance and emissions and it is expected composition variations in the real natural gas will affect our presented results in a similar trend wise-accurate manner. Comparisons will also be made to diesel single injections and split injection cases. Ultimately, this paper aims to quantify methane's effects on engine performance and emissions, adding to the current experimentally derived knowledge of dual fuel combustion.

2. SETUP AND METHODS

2.1 Experimental Setup

The single-cylinder compression ignition research engine from the Advanced Combustion and Energy Systems Laboratory at Stony Brook University is show in Figure 1, with a schematic of the engine setup shown in Figure 2. The engine used for these experiments consists of a Ricardo Hydra research engine block mated to a light-duty 1.7-liter General Motors / Isuzu "Circle-L" 4EE2 aluminum cylinder head with three (3) of the four (4) cylinders de-activated. The glow-plug has been removed and re-bored to retrofit the cylinder pressure transducer. The bowl-in piston geometry and production designed swirl motion enhances fuel-air charge mixing for improved combustion. Additional combustion chamber details are originally provided by Jacobs [32] and Ickes [33]. The engine and direct fuel injector specifications are found in Table 1. To capture performance and emissions data, several sensors are used in the intake, exhaust, coolant, and oil systems. These include K-type thermocouples, pressure gauges, and heaters. For load control, the engine was

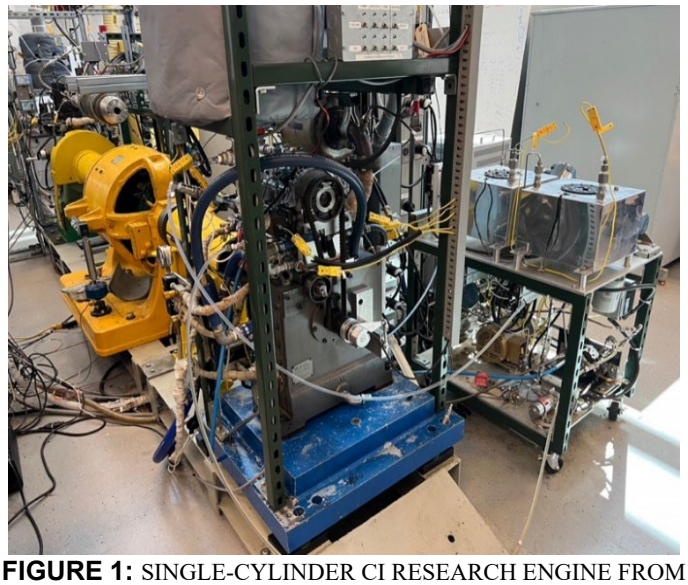

FIGURE 1: SINGLE-CYLINDER CI RESEARCH ENGINE FROM THE ADVANCED COMBUSTION AND ENERGY SYSTEMS LABORATORY AT STONY BROOK UNIVERSITY.

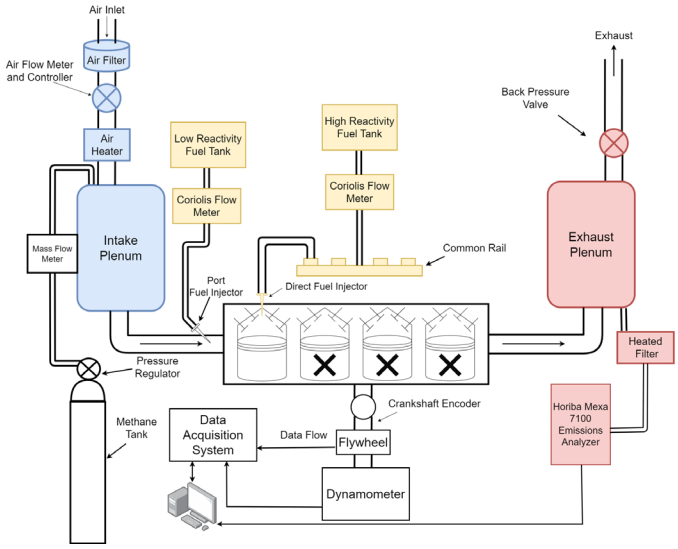

FIGURE 2: EXPERIMENTAL SCHEMATIC ADAPTED FROM HADLICH ET AL. [28] WITH CH4 FUELING SYSTEM ADDED.

coupled to a 30 horsepower General Electric (GE) direct current dynamometer. To regulate the air and methane flow rates, two Alicat mass flow controllers were used. Atmospheric air and methane are then mixed in the intake plenum and delivered to the cylinder via the intake valve. Kistler pressure transducers were used to measure the intake, exhaust, and cylinder pressures. A Kistler crankshaft encoder was used to record crankshaft position. The Kistler tools have a resolution of 0.1 CAD. To determine the air-fuel ratio and measure the oxygen percentage of the exhaust gas, an ECM Lambda CAN module was used. Emissions were measured by a Horiba MEXA 7100DEGR analyzer and a TSI Nanoparticle Emission Tester (NPET) 3795-HC. Together, CO, CO_2, NO_x, total hydrocarbons (THC), and particulate matter (PM) concentration can be recorded. All

sensor data was captured using National Instruments data acquisition (DAQ) boards, which connect to a computer. A custom LabVIEW program reports the sensor values, processes data, and allows for user control of critical engine operations [28]. In this experiment, gaseous methane (CH_4) and research grade No. 2 diesel (DF2) were used. Figure 2 highlights the engine setup schematic.

2.2 Uncertainty Quantification

A degree of uncertainty is present in all experimental work conducted. Anything that is measured with an instrument has an associated percentage of uncertainty as nothing is perfect. In recognizing that this error is present, the uncertainty for each instruments used has been documented in Table 2.

2. 3 Methods

Prior to experimentation, the engine was warmed up to operating temperature. Intake pressure and temperature were held steady at ambient conditions ranging from 315-317 K and 94-100 kPa, respectively. Three combustion cases were investigated, diesel single injection, diesel split injection (pilot and main) and finally methane with diesel pilot injection, with

TABLE 1: ENGINE AND INJECTOR SPECIFICATIONS BY RAN ET AL. [27] AND RISTOW HADLICH ET AL. [28].

General Specifications and Parameters	
Number of cylinders	1
Number of valves per cylinder	4
Strokes per cycle	4
Bore	79 millimeters (mm)
Stroke	86 millimeters (mm)
Connecting rod length	160 millimeters (mm)
Total displaced volume	0.4215 liters (L)
Geometric compression ratio	15.1:1
Intake valve opening (IVO)	354° before TDC
Intake valve closing (IVC)	146° before TDC
Exhaust valve opening (EVO)	122° after TDC
Exhaust valve closing (EVC)	366° after TDC
Engine speed	1200 RPM
Air flow rate set point	400 SLPM
Direct injection pressure	750 bar
Direct injector location	Centrally mounted
Number of injector nozzle holes	6
Nozzle diameter	130 micrometers (μm)
Maximum injector pressure	≤ 2000 bar
Injector spray induced angle	150 degrees
Injector spray type	Solid cone spray

the procedure for data collection as follows. For the diesel single injection cases, once pseudo-steady operating conditions were achieved, an equivalence ratio sweep was done by increasing the injection duration time which ranged from 0.340 – 0.460 milliseconds (ms). For each equivalence ratio, injection timing was swept to find maximum break torque (MBT). The data for each MBT was saved. For split diesel injection, after reaching pseudo-steady conditions, an equivalence ratio sweep is performed, with each case recorded being the injection timing

TABLE 2: EQUIPMENT MEASUREMENT RANGES AND UNCERTANTIES AS DETAILED BY RAN ET AL. [29].

Measurement	Instrument	Range	Uncertainty
Intake Pressure	Kistler 4011A	0 – 5 bar	≤ ± 0.5%
Cylinder Pressure	Kistler 6045B	0 – 250 bar	≤ ± 0.3%
Exhaust Pressure	Kistler 4049B	0 – 5 bar	≤ ± 0.5%
Crankshaft Encoder	Kistler 2614C11	0 – 12,000 RPM	≤ ± 0.00007
Signal Amplifier	Kistler 4665B	Not Applicable	≤ ± 0.3%
Dynamometer	GE Electric Dynamometer	0 – 4,500 RPM	≤ ± 0.1%
Lambda (O_2) Sensor	ECM Lambda CAN Module	ϕ: 0.04 – 2.5	≤ ± 0.9%
Flow Meter	Micromotion	0 – 40.9 kg/h	≤ ± 0.1% liquid flow
Methane Mass Flow	Alicat MCRWH-100SLPM-D/5M	0.01 – 100 SLPM	± (≤ 0.8% reading + ≤ 0.2% full scale)
Air Mass Flow	Alicat MCRWH-1000SLPM-D/5M	0.1-1000 SLPM	± (≤ 0.8% reading + ≤ 0.2% full scale)
Type K Thermocouple	Omega Engineering	-200°C to 1,250°C	≤ ± 0.75% reading
CO Emissions	Horiba MEXA 7100	0 – 5,000 ppm	≤ ± 1.0%
CO_2 Emissions	Horiba MEXA 7100	0% – 15%	≤ ± 1.0%
NO_x Emissions	Horiba MEXA 7100	0 – 3,000 ppm	≤ ± 1.0%
O_2 Emissions	Horiba MEXA 7100	0% – 18%	≤ ± 1.0%
THC Emissions	Horiba MEXA 7100	0 – 10,000 ppm	≤ ± 1.0%
PM Emissions	TSI Nanoparticle Emission Tester (NPET) 3795-HC	< 50% at 23 nm and > 50% at 41 nm for Solid particles from 23 nm to 1,000 nm	≤ ± 10%

that resulted in MBT. The duration of pilot injection for all split injection cases was held constant at 0.130 ms with the main injection duration being used to change the ϕ. The main injection duration ranged from 0.320 – 0.590 ms. The process for recording methane with diesel pilot injection cases is similar to the split case with a pilot injection duration of 0.140 ms. To control the equivalence ratio for these cases, rather than adjust the duration of main injection, the set point of the methane flow meter was changed to allow for flows from 15 standard liters per minute (SLPM) up to 22.5 SLPM. To summarize, for all three cases, the equivalence ratio is swept, where for each equivalence ratio the injection timing that results in the highest MBT is recorded. This is done for all equivalence ratios possible, until the knock limit is reached. For all cases, the injection pressure was set to 750 bar. For each operating point, 300 cycles of that point are saved which are then fed and analyzed for heat release using an in-house MATLAB code.

3. RESULTS AND DISCUSSION

3.1 Summary of Cases

A series of 22 experimental combustion conditions were run spanning from five baseline injection diesel cases, eight split injection (pilot and main) diesel cases and nine diesel pilot with methane fumigation cases. The combustion conditions, including energy-based blend ratio, and resulting $IMEP_{gross}$ is tabulated below in Table 3. The diesel energy content is the percentage of total energy input that comes from diesel. For the split injection case, the percentage is provided as percentage of energy from pilot injection/ percentage from main injection. The percentage of energy from methane as well as the total energy input from fuel is provided.

Gross indicated mean effective pressure, $IMEP_{gross}$, is the gross work produced by the engine, normalized to the displaced volume of the engine. Normalizing work with respect to volume allows for fair comparison of this engine's work output at these combustion conditions to other engines of varying sizes. The cases that produced the highest $IMEP_{gross}$ are written in bold. Table 3 shows that methane resulted in the highest $IMEP_{gross}$ at $\phi = 0.90$ and SOI of 5 CAD before TDC.

When comparing diesel split injection and methane at both $\phi \approx 0.6$ and $\phi \approx 0.7$, $IMEP_{gross}$ was higher in the methane cases with a difference of 5.3% and 4.2%, respectively. Diesel single injection was knock limited and was not able to reach higher equivalence ratios for a fair comparison to be made. It is interesting to note that for the methane with diesel pilot cases, as SOI approached TDC, at a constant ϕ, the $IMEP_{gross}$ decreased

TABLE 3: IMEP AND RESPECTIVE COMBUSTION PARAMETERS FOR ALL CASES

Fuel	Equiv. Ratio [ϕ]	Pilot SOI (aTDC) [°]	Main SOI (aTDC) [°]	Total Input Fuel Energy [J]	Diesel Energy Content [%]	CH_4 Energy Content [%]	$IMEP_g$ [bar]
Diesel Single Inj.	0.20	-	-4	242.40	100	-	1.55
	0.25	-	-2.5	301.70	100	-	2.29
	0.29	-	-1	349.67	100	-	2.84
	0.37	-	0	433.50	100	-	3.76
	0.42	**-**	**1**	**507.68**	**100**	**-**	**4.24**
Diesel Split Inj.	0.20	-10	-6	244.05	22.8 / 77.2	-	1.46
	0.24	-8	-4	294.15	22.3 / 77.7	-	1.99
	0.26	-6	-2	306.50	21.8 / 78.2	-	2.32
	0.31	-4	0	369.75	20.9 / 79.1	-	3.03
	0.37	-2	2	441.35	19.7 / 80.3	-	3.72
	0.45	0	4	541.63	18.9 /81.1	-	4.55
	0.58	2	6	691.43	17.3 / 82.7	-	5.74
	0.73	**4**	**8**	**869.30**	**15.9 / 84.1**	**-**	**6.68**
CH_4 w/ Diesel Pilot	0.61	-8	fumigated	716.74	52.7	47.3	6.06
	0.72	-7	fumigated	819.26	51.6	48.4	6.97
	0.80	-5	fumigated	902.59	49.9	50.1	7.67
	0.90	**-5**	fumigated	**991.9**	**48.8**	**51.2**	**8.33**
	0.89	-4	fumigated	985.56	48.4	51.6	8.32
	0.89	-3	fumigated	982.38	48.3	51.7	8.27
	0.89	-2	fumigated	984.80	48.3	51.7	8.23
	0.89	-1	fumigated	988.20	48.6	51.4	8.09
	0.90	0	fumigated	996.52	49	51.0	7.72

with a 7.3% decrease between SOI of 5 and 0 CAD bTDC. This indicates that for more efficient combustion to take place, the pilot injection of diesel needs to be advanced.

3.2 Cylinder Pressure and Heat Release Analysis

Pressure traces are foundational to engines research, all work-based analysis including mean effective pressures and efficiencies rely on pressure traces. The mean filtered pressure traces plotted in Figure 3 include: the richest equivalence ratios for diesel single and split injection which are 0.42 and 0.73 respectively, as well as the pressure trace for methane with diesel pilot injection for ϕ = 0.9 and SOI ranging from -5 to 0 CAD aTDC and ϕ = 0.7 at SOI of –7 CAD aTDC. The corresponding apparent gross heat release profiles are shown in Figure 4. The cylinder pressure profile shows two distinct peaks which is an expected result for the experimental conditions evaluated. The first peak is from the initial compression of the cylinder contents, and the second peak is due to the pressure rise associated with the energy released from the combustion of the air-charge mixture.

For the methane with diesel pilot cases at an equivalence ratio of 0.9, it can be observed that by advancing the SOI, peak cylinder pressure and heat released rate are both increased. Further, the higher chamber temperatures associated with the higher cylinder pressures at earlier SOI timings result in faster, more reactive fuel chemistry, given the Arrhenius dependence on temperature, and an increased laminar flame speed explaining the increase in peak magnitude and decrease in heat release profiles observed.

Subsequently, the ignition delay, the period between SOI and SOC, is decreased with advancing diesel pilot injection timings for the CH_4 combustion cases when comparing Figure 3 and Figure 4. Also note that as injection timings for the diesel pilot are retarded in the methane combustion cases, and the combustion event gets phased further into the expansion stroke and produces lower peak cylinder pressures. As the combustion chamber volume expands, the turbulence intensity in the chamber decreases, causing the flame propagation to decrease, thus requiring longer durations for the combustion event to complete, as seen in Figure 4. On the contrary, as SOI timings for the diesel pilot of the methane combustion is advanced, the burn duration is decreased.

In classical split injection diesel only combustion, the pilot injection prepares the chamber for the main injection by allowing a small amount of diesel fuel to burn and release energy and thus increase the overall temperature conditions that the main charge will experience. The increased temperature reduces the ignition delay period for the main injection because of the more favorable spray vaporization conditions and ever so slightly more reactive chemical kinetics, which, in turn, reduces the portion of the fuel charge encumbered with the premixed burn and allows main charge to transition sooner to diffusion burn.

In the case of a methane combustion with diesel pilot, the diesel pilot behaves in a similar fashion as described above, but the secondary injection does not need to happen as the methane was fumigated in the intake manifold and inducted over the

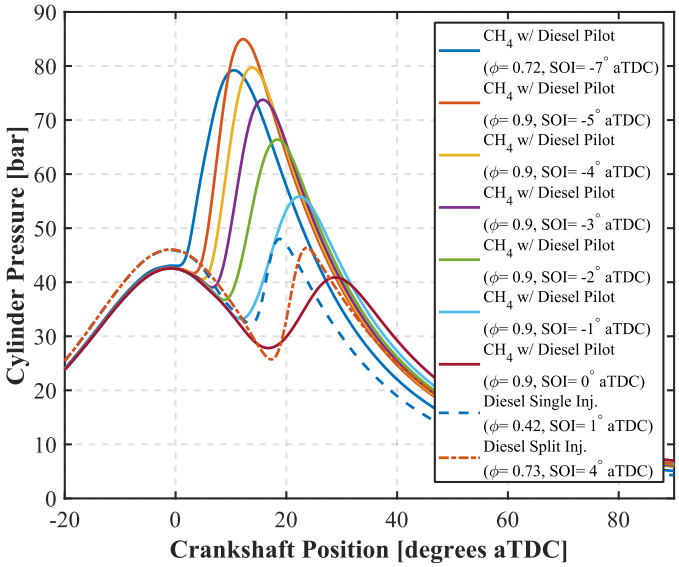

FIGURE 3: CYLINDER PRESSURE PLOTTED AGAINST CRANK ANGLE DEGREE FOR DIESEL SINGLE INJECTION, SPLIT INJECTION AND DIESEL PILOT INJECTION WITH METHANE

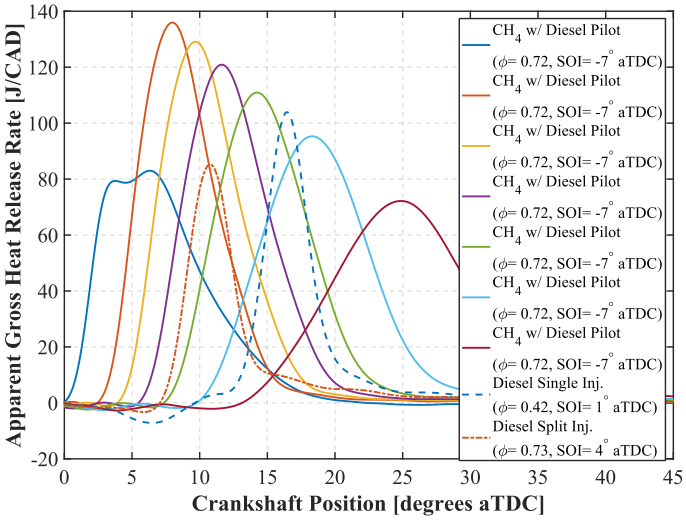

FIGURE 4: HEAT RELEASE RATE PLOTTED AGAINST CRANK ANGLE DEGREE FOR DIESEL SINGLE INJECTION, SPLIT INJECTION AND DIESEL PILOT INJECTION WITH METHANE

intake during the cylinder filling. Thus, the diesel pilot acts as the ignition source for the methane combustion, which follows the entrainment and burn-up phenomenological combustion model, which has classically been reserved for spark-ignited engines.

When comparing the split injection diesel case (ϕ = 0.73) to a similar energy input (see Table 3) case of methane with pilot diesel (ϕ = 0.72), the methane case is able to achieve a much higher peak pressure than the split injection pure diesel case as seen in Figure 3. This can be attributed to the timing and shape of the apparent heat release rate profile, shown in Figure 4, and

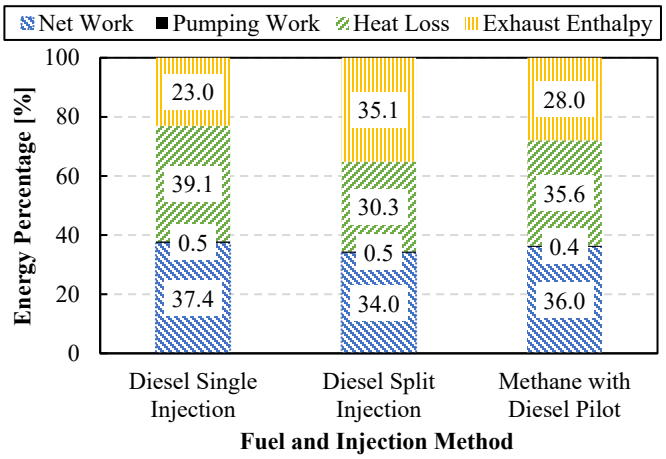

FIGURE 5: ENERGY BREAKDOWN FOR RICHEST CASES FOR EACH COMBUSTION MODE.

the reduction in ignition delay time due to the advancing diesel pilot. Therefore, the methane with diesel pilot case has much sooner heat release, earlier in the expansion stroke, thus the peak pressures achieved are higher than the comparative diesel split-injection case. This relationship between heat released rate and peak pressures is also demonstrated in Figures 3 and 4.

For maximizing power output and increased phasing controllability, shorter burn durations and therefore higher peak pressures and shorter ignition delay time is desirable; so, when comparing methane with diesel pilot injection cases at a constant ϕ, an advanced start of injection timing is necessary and desired.

Energy flows have been previously evaluated by Yang et al. [34] for reactivity studies on this engine architecture and have inspired a similar analysis to be performed for this study. Figure 5 shows the output energy breakdown for an input total heat released for the richest equivalence ratio for each case. The combustion parameters for each case are as follows: single diesel injection at a ϕ = 0.42 and SOI = 1 CAD aTDC, split diesel injection with a ϕ = 0.73 and SOI = 4 CAD aTDC and methane with a diesel pilot with a ϕ = 0.90 and SOI = -5 CAD aTDC. The total heat released is assumed to follow the following equation and be transformed into the four plotted categories which are net work, pumping work, heat loss and exhaust enthalpy.

$$Total\ Heat\ Released = W_{net} + W_{pumping} + Q_{loss} + Exhaust\ Enthalpy \quad \text{(Eq. 1)}$$

The heat released is found using the application of the first law of thermodynamics. The net and pumping work is calculated by integrating pressure with respect to change in volume. The heat loss is found based on surface area of cylinder, the bulk cylinder temperature and the convective coefficient of heat transfer which is derived using Woschni equation. Finally, the remaining percentage of energy left is assumed to exit the engine as enthalpy of the exhaust and is found using equation 1. There are other energy paths that can occur, however, for the purpose of this graph all other pathways have been grouped with the enthalpy in the calculations performed. The pumping work was negligible in all cases. By looking at Figure 5, on a percentage basis we can see that diesel single injection produces the most work followed by methane with diesel pilot and then diesel split injection. Methane can produce similar relative net work outputs which is a good indication that methane is a viable replacement energy source. The overall heat losses and exhaust enthalpy of the methane with diesel pilot case are in between the single and split diesel cases, showing overall on an energy percentage basis that methane can produce similar energy breakdown outputs.

3.2 Combustion Investigation & Performance Trends

With the introduction of a new fuel and different injection events, an analysis into how this has affected the combustion process inside the chamber was performed. An interesting comparison to make is the variation of start of combustion with respect to start of injection which is plotted in Figure 6. In this study, the SOC is defined as the first crank angle degree where the derivative of the heat release rate is consistently positive within a rolling window of 3.5 CAD. In both diesel cases, there is a linear relationship between SOI and SOC, showing that as SOI is advanced so is SOC. Methane follows this trend for earlier injection timings, however, as SOI is retarded it begins to deviate and demonstrate a more non-linear correlation. From this plot, the ignition delay period is calculated and also plotted in Figure 6. Methane's ignition delay period rises non-linearly with respect to SOI. This can be in part attributed to the alternate mode of combustion that methane undergoes compared to the two diesel cases. The two diesel cases are undergoing purely compression ignition whereas with the methane case, it is being ignited by the diesel pilot injection which is acting like a spark plug. In general, the start of injection phasing is a good control for the start of combustion for the range of conditions studied.

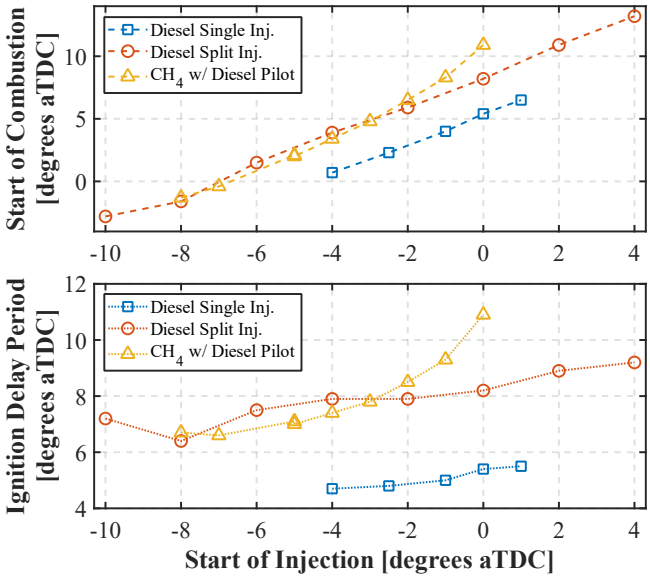

FIGURE 6: START OF COMBUSTION AND IGNITION DELAY VARIATION AS A FUNCTION OF START OF INJECTION.

Another important set of metrics to analyze when discussing the combustion of different fuel types and combustion modes are the combustion efficiency, gross thermal efficiency, and gross indicated fuel conversion efficiency. Combustion efficiency is the measure of consumed fuel energy input and is directly calculated by the emission analyzer based on the measured gaseous species in the exhaust stream. Figure 7 shows efficiency above 93% in all tested scenarios, and generally increased as SOI was retarded. Gross indicated thermal efficiency (Figure 8) is the ratio of the gross indicated work to the heating energy of the fuel inputted. For both diesel cases, a peak in efficiency with SOI at or near TDC was observed and was reduced at earlier or later injection timings. This contrasts with methane, which decreased as injection was retarded. This implies that for the most effective conversion of chemical energy stored in the fuel to work output

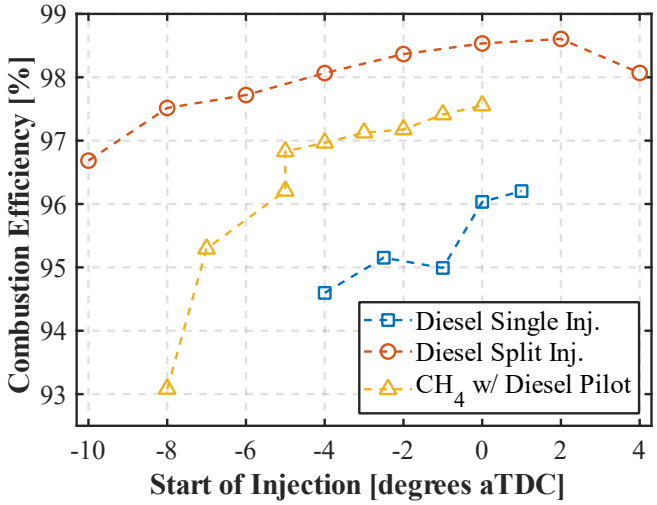

FIGURE 7: COMBUSTION EFFICIENCY VARIATION AS A FUNCTION OF START OF INJECTION.

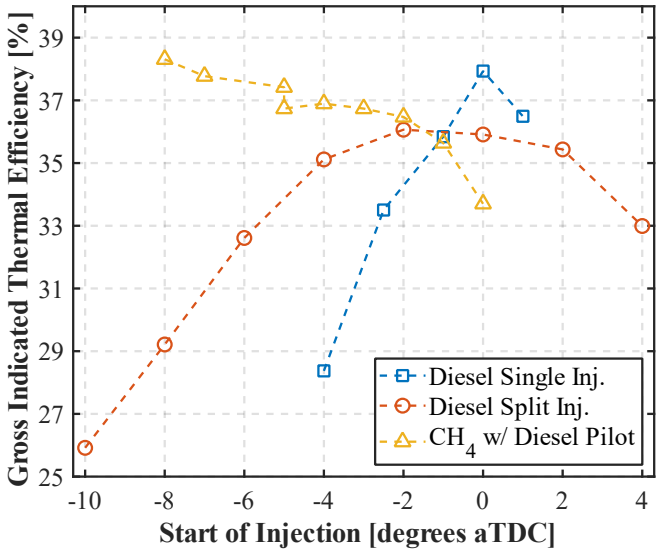

FIGURE 8: GROSS INDICATED THERMAL EFFICIENCY VARIATION AS A FUNCTION OF START OF INJECTION.

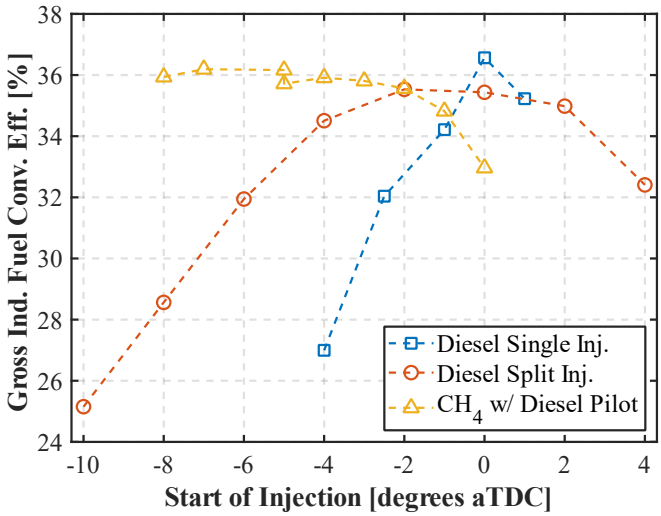

FIGURE 9: GROSS INDICATED FUEL CONVERSION EFFICIENCY VARIATION AS A FUNCTION OF START OF INJECTION.

for the methane cases happens at earlier SOI timings. This is confirmed by the IMEP values tabulated earlier where the gross IMEP decreased with retarded SOI.

Gross indicated fuel conversion efficiency ($\eta_{f,ig}$), shown in Figure 9, is determined by directly calculating the gross work from the indicated pressure measurements and assumed swept displacement volume as well as the determination of the total fuel energy input based on fuel flow rate measurements. This efficiency shows identical trends to Figure 8, at earlier SOI, methane outperforms both diesel cases.

In general, for methane to be a viable alternative fuel, it needs to produce similar efficiencies to that of diesel. In most cases for the methane with pilot injection it was able to perform as efficient if not more efficient than the diesel; particularly when looking at gross indicated thermal efficiency and gross indicated fuel conversion efficiency, methane was able to outperform both diesel cases for an SOI timing from -8 to -3 degrees aTDC.

3.3 Emissions Characterization

When evaluating any low-carbon alternative fuel, emissions are at the forefront of consideration. The emission species that were measured are CO, CO_2, NO_x, THC, and particulate matter. Figures 10-12 depict the emission species in grams per kilogram of fuel input relative to equivalence ratio. The value of this representation is to normalize and compare the emissions on a fuel mass basis. For all plots in this section, points are an average of pseudo-steady data. The dashed lines represent interpolated values between the points.

The first observation from these figures is that lower levels of CO, NO_x, and THC were generated with a diesel single injection across the equivalence ratio sweep. This is because the tested equivalence ratios were all ran lean and with a high combustion efficiency, there are little incomplete combustion products to be detected. Since combustion efficiency increased with equivalence ratio, it is expected that CO levels decreased as seen

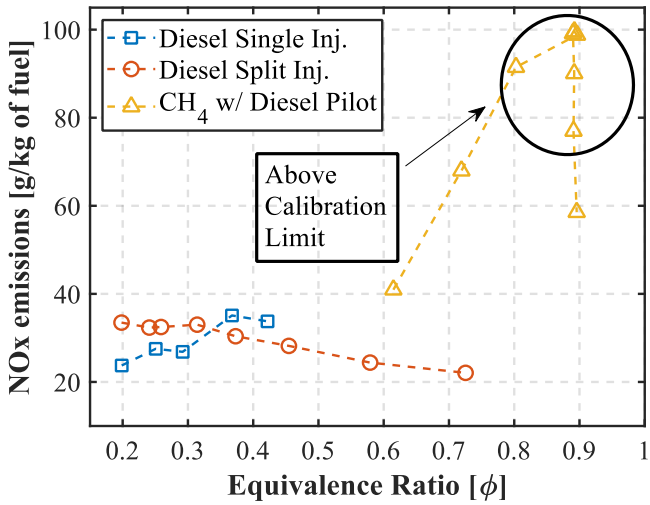

FIGURE 10: NO_x EMISSIONS WITH RESPECT TO EQUIVALENCE RATIO.

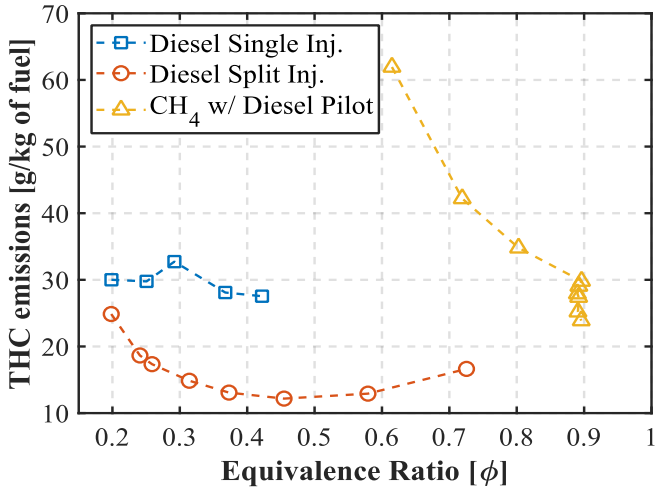

FIGURE 11: THC EMISSIONS WITH RESPECT TO EQUIVALENCE RATIO.

in Figure 12. There is a slight decrease in CO_2 levels as equivalence ratio increases. When testing diesel split injection, a similar trend emerged, where minimal CO, NO_x, and THC was measured. CO_2 showed a slightly larger increase than diesel single injection, reaching a peak at its richest case.

Finally, the methane with diesel pilot injection emissions is also plotted on Figures 10-12. Some things to note are the overall high NO_x emissions for all runs. The cases within the circle in Figure 10 were measurements of NO_x above the calibration limit of the Horiba MEXA 7100. The line of constant equivalence ratio in Figure 10 was the SOI timing sweep done for the methane with diesel pilot case. This line demonstrates the effect of SOI on NO_x emissions, where later timings can almost halve the amount of NO_x produced. Other emissions to make note of is the large decrease in THC with respect to equivalence ratio. CO remained relatively constant with respect to equivalence ratio and CO_2 showed a steady increase with no change with respect to SOI demonstrated by collection of points at φ=0.9.

The soot-NO_x tradeoff should be considered when analyzing emissions produced by a diesel engine. Within specific bounds of equivalence ratio and cylinder temperature, either more particulate matter or NOx will be emitted. The best strategy to minimize these harmful pollutants is to use lean, low temperature combustion [35-37], but this may result in reduced output at atmospheric intake conditions.

This trade off can be seen in the ϕ = 0.90 and a SOI of 5 CAD bTDC case, where an in-cylinder temperature is determined to be 2339 K using the ideal gas law, the in-cylinder pressure measurement, displaced volume calculated from geometrical relationships, and determination of the working fluid on a crank angle resolved basis. The NOx emission percentage for this case was an order of magnitude greater than that of the diesel case whose temperatures for all cases never exceeded 2000 K.

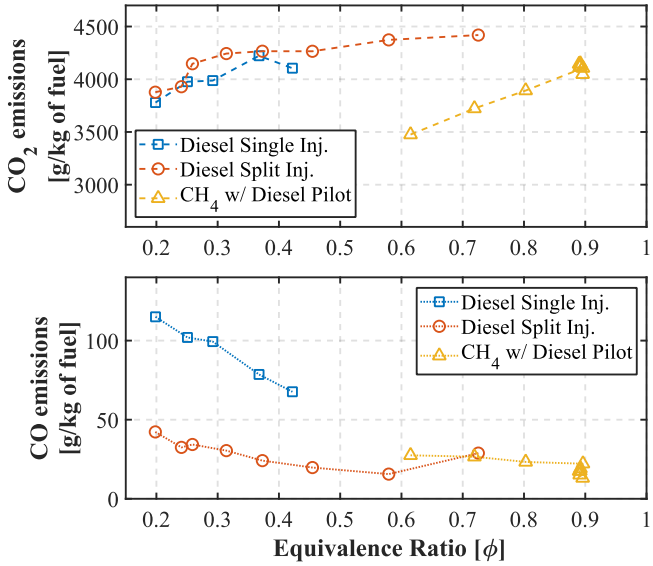

FIGURE 12: CO AND CO_2 EMISSIONS WITH RESPECT TO EQUIVALENCE RATIO

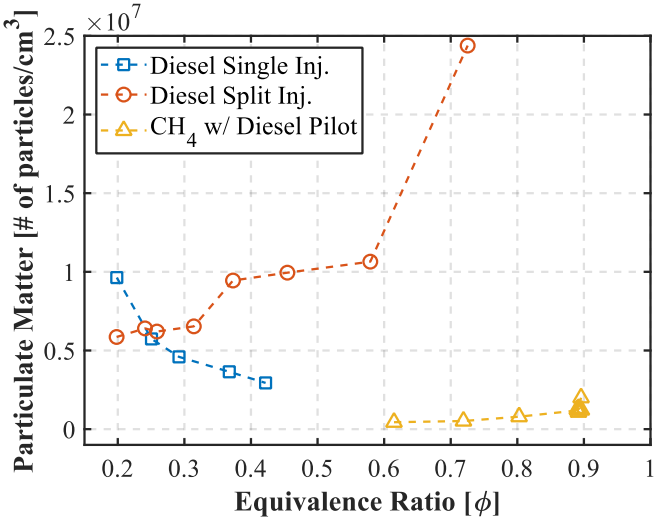

FIGURE 13: PARTICULATE MATTER EMISSIONS WITH RESPECT TO EQUIVALENCE RATIO.

a solution to this trade-off is to use an aftertreatment device, such as a catalytic converter, to help reduce the tailpipe emissions [38]. Figure 13 follows the trend of the soot-NOx tradeoff as methane produces the least amount of particulate matter.

For single injection diesel particulates produced decreases with respect to increasing equivalence ratio and for split injection it increases. For a ϕ =0.7, comparing diesel split and methane particulate production, diesel split produces 46.7 times more particulate matter than methane, who for all cases produced a number concentration of 25 particles/cm^3 or less. Additionally, for methane cases with ϕ =0.9 and different SOI, we see relatively no change in particulate production showing that there is some flexibility in operating points for methane.

4. CONCLUSIONS

In this experimental investigation, a compression ignition research engine was used to evaluate the effects of equivalence ratio and injection timing on performance and emissions during the diesel pilot assisted combustion of methane fuel. Through analysis of the cylinder pressure trace, heat release rate, performance trends, and an emission characterization, comparisons were made to a baseline single and split diesel injection strategy. The key conclusions of this study are as follows:

- Dual fuel combustion utilizing a diesel pilot to ignite a methane fuel-air charge mixture in a compression ignition engine was successfully achieved.
- The fuel source, equivalence ratio, and injection timing which provided the most optimal balance of engine performance and engine-out emissions was found to be methane with a diesel pilot, at $\phi = 0.90$, and injection at 5 CAD before TDC, respectively.
- When comparing peak cylinder pressure between methane with diesel pilot and diesel split injection for the same equivalence ratio, it was found that methane was able to produce a 41.49% higher pressure than diesel split injection.
- As the start of injection was brought closer to TDC, peak $IMEP_{gross}$, and heat release rate decreased and occurred later in the engine cycle.
- Methane combustion was able to convert 36% of all total heat released to net work, converting a high percentage of energy to work than compared to the diesel split injection.
- At similar equivalence ratios, methane was capable of similar engine performance and efficiencies as diesel split injection.
- Methane with a diesel pilot reduced CO emissions by 7.9%, at the expense of 207.9% and 153.8% higher NO_x and THC emissions respectively when compared to diesel split injection at $\phi \approx 0.7$.
- Timing of the pilot injection was found to be an effective method for controlling the start of methane combustion.

Methane, the primary component of natural gas, performed sufficiently in comparison to single and split injections of research grade No. 2 diesel (DF2). Some disadvantages when using methane as an alternative fuel were found, but they do not outweigh the benefits. The findings of this paper can recommend natural gas as an alternative fuel, which has the potential to prolong the usefulness of the internal combustion engine in its many applications as the world enters a climate conscious era. Future experiments should focus on additional comparison and quantification of diesel piloted methane over a broader operating range and consider the use of green hydrogen blending with the methane for the main fuel event.

ACKNOWLEDGEMENTS

This work was made possible through funding from the U.S. Office of Naval Research under Award No. N00014-22-1-2001.

REFERENCES

[1] EPA. “Inventory of U.S. Greenhouse Gas Emissions and Sinks: 1990-2020.” Technical Report No. EPA 430-R-22-003. U.S. Environmental Protection Agency, Washington, D.C. https://www.epa.gov/system/files/documents/2022-04/us-ghg-inventory-2022-main-text.pdf.

[2] EIA. “Natural gas explained.” U.S. Energy Information Administration, Washington, D.C. https://www.eia.gov/energyexplained/natural-gas/.

[3]“Learn about Natural Gas.” *Enbridge*, www.enbridgegas.com/about-enbridge-gas/learn-about-natural-gas. Accessed 1 July 2023.

[4] Speight, James G. *Natural Gas: A Basic Handbook*. Second ed., Gulf Professional Publishing, 2019.

[5] Kumar, Satish, Kwon, Hyouk-Tae, Choi, Kwang-Ho, Lim, Wonsub, Cho, Jae Hyun, Tak, Kyungjae, and Moon, Il. “LNG: An eco-friendly cryogenic fuel for sustainable development.” *Applied Energy* Vol. 88 No. 12 (2011): pp. 4264-4273. DOI 10.1016/j.apenergy.2011.06.035. https://doi.org/10.1016/j.apenergy.2011.06.035.

[6] DOE. “Natural Gas Vehicles.” U.S. Department of Energy, Washington, D.C. https://afdc.energy.gov/vehicles/natural_gas.html.

[7] Ahmad, Zeeshan, Kaario, Ossi, Qiang, Cheng, and Larmi, Martti. “Effect of pilot fuel properties on lean dual-fuel combustion and emission characteristics in a heavy-duty engine.” Applied Energy Vol. 242 (2021). DOI 10.1016/j.apenergy.2020.116134. https://doi.org/10.1016/j.apenergy.2020.116134.

[8] Ahmad, Zeeshan, Kaario, Ossi, Qiang, Cheng, Vuorinen, Ville, and Larmi, Martti. “A parametric investigation of diesel/methane dual-fuel combustion progression/stages in a heavy-duty optical engine.” Applied Energy Vol. 251 (2019). DOI 10.1016/j.apenergy.2019.04.187. https://doi.org/10.1016/j.apenergy.2019.04.187.

[9] Tiwari, Abhay. “Converting a Diesel Engine to Dual-Fuel Engine Using Natural Gas.” *International Journal of Energy Science and Engineering* Vol. 1 No. 5 (2015): pp. 163-169. DOI 10.13140/RG.2.2.29781.93926.

https://doi.org/10.13140/RG.2.2.29781.93926.

[10] Wagemakers, A. and Leermakers, C. "Review on the Effects of Dual-Fuel Operation, Using Diesel and Gaseous Fuels, on Emissions and Performance." Technical Report No. SAE Technical Paper 2012-01-0869. Eindhoven University of Technology, Eindhoven, Netherlands. 2012. DOI 10.4271/2012-01-0869. https://doi.org/10.4271/2012-01-0869.

[11] Shatrov, Mikhail G., Sinyavski, Vladimir V., Dunin, Andrey Yu., Shishlov, Ivan G., and Vakulenko, Andrey V. "Method of Conversion of High- and Middle-Speed Diesel Engines into Gas Diesel Engines." Mechanical Engineering Vol. 15 No. 3 (2017): pp. 383-395. DOI 10.22190/FUME171004023S. https://doi.org/10.22190/FUME171004023S.

[12] Weaver, Christopher S., and Turner, Sean H. "Dual Fuel Natural Gas/Diesel Engines: Technology, Performance, and Emissions." Technical Report No. SAE Technical Paper 940548. 1994. DOI 10.4271/940548. https://doi.org/10.4271/940548.

[13] Taniguchi, Satoshi, Masubuchi, Masahiko, Kitano, Koji, and Mogi, Kazuhisa. "Feasibility Study of Exhaust Emissions in a Natural Gas Diesel Dual Fuel (DDF) Engine." Technical Report No. SAE Technical Paper 2012-01-1649. 2012. DOI 10.4271/2012-01-1649. https://doi.org/10.4271/2012-01-1649.

[14] Caris, D. and Nelson, E. "A New Look at High Compression Engines." Technical Report No. SAE Technical Paper 590015. 1959. DOI 10.4271/590015. https://doi.org/10.4271/590015.

[15] Raine, R. R., Stephenson, J., and Elder, S. T. "Characteristics of Diesel Engines Converted to Spark Ignition Operation Fuelled with Natural Gas." Technical Report No. SAE Technical Paper 880149. University of Auckland, Auckland, New Zealand. 1988. DOI 10.4271/880149. https://doi.org/10.4271/880149.

[16] Thermo Power Corporation, Tecogen Division. "Conversion of a Diesel Engine to a Spark Ignition Natural Gas Engine." Technical Report No. NREL/TP-425-21682. U.S. Department of Energy, Washington, D.C. DOI 10.2172/390571. https://doi.org/10.2172/390571.

[17] Liu, Jinlong and Dumitrescu, Cosmin E. "Methodology to separate the two burn stages of natural-gas lean premixed-combustion inside a diesel geometry." *Energy Conversion and Management* Vol. 195 (2019): pp. 21-31. DOI 10.1016/j.enconman.2019.04.091. https://doi.org/10.1016/j.enconman.2019.04.091.

[18] Ismail, Muammar Mukhsin, Zulkifli, Fathul Hakim, Fawzi, Mas, and Osman, Shahrul Azmir. "Conversion Method of a Diesel Engine to a CNG-Diesel Dual Fuel Engine and its Financial Savings." *ARPN Journal of Engineering and Applied Sciences* Vol. 11 No. 8 (2016). DOI 10.59018/arpn. https://doi.org/10.59018/arpn.

[19] Liu, Zongkuan, Zhou, Lei, Liu, Bo, Zhao, Wanhui, and Wei, Haiqiao. "Effects of equivalence ratio and pilot fuel mass on ignition/extinction and pressure oscillation in a methane/diesel engine with pre-chamber." *Applied Thermal Energy* Vol. 158 (2019): pp. 113777. DOI 10.1016/j.applthermaleng.2019.113777. https://doi.org/10.1016/j.applthermaleng.2019.113777.

[20] Tripathi, Gaurav, Sharma, Priybrat, and Dhar, Atul. "Computational study of diesel injection strategies for methane-diesel dual fuel engine." *Cleaner Engineering and Technology* Vol. 6 (2022): pp. 100393. DOI 10.1016/j.clet.2021.100393. https://doi.org/10.1016/j.clet.2021.100393.

[21] Yousefi, Amin, Birouk, Madjid, and Guo, Hongsheng. "An experimental and numerical study of the effect of diesel injection timing on natural gas/diesel dual-fuel combustion at low load." *Fuel* Vol. 203 (2017): pp. 642-657. DOI 10.1016/j.fuel.2017.05.009. https://doi.org/10.1016/j.fuel.2017.05.009.

[22] Mansour, Cheikh, Bounif, Abdelhamid, Aris, Abdelkader, and Gaillard, Françoise. "Gas–Diesel (dual-fuel) modeling in diesel engine environment." *International Journal of Thermal Sciences* Vol. 40 No. 4 (2001): pp. 409-424. DOI 10.1016/S1290-0729(01)01223-6. https://doi.org/10.1016/S1290-0729(01)01223-6.

[23] DOE. "Renewable Natural Gas Production." U.S. Department of Energy, Washington D.C. https://afdc.energy.gov/fuels/natural_gas_renewable.html.

[24] Barik, Debabrata, Satapathy, Ashok Kumar, and Murugan S. "Combustion analysis of the diesel–biogas dual fuel direct injection diesel engine – the gas diesel engine." *International Journal of Ambient Energy* Vol. 38 No. 3 (2017): pp. 259-266. DOI 10.1080/01430750.2015.108668. https://doi.org/10.1016/S1290-0729(01)01223-6.

[25] Shaalan, Amr, Nasim, Md Nayer, Mack, J. Hunter, Van Dam, Noah, and Assanis, Dimitris. "Understanding Ammonia / Hydrogen Fuel Combustion Modeling in a Quiescent Environment", ICEF2022-91185, ASME ICE Forward, 2022. DOI 10.1115/ICEF2022-91185. https://doi.org/10.1115/ICEF2022-91185.

[26] Nasim, Md Nayer, Nawaz, Behlol, Kanti Das, Shubhra, Lan-dis, Joshua, Shaalan, Amr, Van Dam, Noah, Pablo Trelles,Juan, Assanis, Dimitris and Mack, J. Hunter. "Investigation of the Laminar Burning Velocity and Exhaust Charac-teristics of Methane-Ammonia-Hydrogen Ternary Blends." Internal Combustion Engine Division Fall Technical Conference. 2023. DOI 10.1115/ICEF2023-109918.

[27] Ran, Zhongnan, Ristow Hadlich, Rodrigo, Yang, Ruinan, Dayton C., David, Mante D., Ofei, and Assanis, Dimitris. "Experimental investigation of naphthenic biofuel surrogate combustion in a compression ignition engine." *Fuel* Vol. 312 (2022): pp.122868. DOI 10.1016/j.fuel.2021.122868. https://doi.org/10.1016/j.fuel.2021.122868.

[28] Ristow Hadlich, Rodrigo, Ran, Zhongnan, Yang, Ruinan, Assanis, Dimitris, Mante, Ofei, and Dayton, David. "Experimental Investigation and Comparison of a Decalin/Butylcyclohexane Based Naphthenic Bio-Blendstock Surrogate Fuel in a Compression Ignition Engine." *SAE International Journal of Advances and Current Practices in Mobility* Vol. 4 No. 5 (2022): pp. 1771-1781. DOI 10.4271/2022-01-0513. https://doi.org/10.4271/2022-01-0513.

[29] Ristow Hadlich, Rodrigo, Ran, Zhongnan, Yang, Ruinan, Mante, Ofei, Dayton, David, and Assanis, Dimitris

"Experimental Investigation of a Butylcyclohexane / Propylcyclohexane Based Naphthenic Bio-Blendstock Surrogate Fuel for Use in a Compression Ignition Engine", Internal Combustion Engine Division Fall Technical Conference. 2023. DOI 10.1115/ICEF2023-110527.

[30] Hammond, Zachary M., John H. Mack, and Robert W. Dibble. "Effect of hydrogen peroxide addition to methane fueled homogeneous charge compression ignition engines through numerical simulations." *International Journal of Engine Research* Vol. 17, No. 2 (2016): pp. 209-220. DOI 10.1177/1468087414564230. https://doi.org/10.1177/1468087414564230.

[31] Kakaee, Amir-Hasan, Rahnama, Pourya, and Paykani, Amin. "The Influence of Fuel Composition on the Combustion and Emission Characteristics of Natural Gas Fueled Engines." *Renewable and Sustainable Energy Reviews* Vol. 38, (2014): pp. 64–78. DOI 10.1016/j.rser.2014.05.080. https://doi.org/10.1016/j.rser.2014.05.080.

[32] Jacobs, T. "Simultaneous Reduction of Nitric Oxide and Particulate Matter Emissions from a Light-Duty Diesel Engine Using Combustion Development and Diesel Oxidation Catalyst". Dissertation. University of Michigan. Ann Arbor. 2005.

[33] Ickes, A.M. "Fuel property impact on a premixed diesel combustion mode". Dissertation. University of Michigan. Ann Arbor. 2009.

[34] Yang, Ruinan, Ran, Zhongnan, Ristow Hadlich, Rodrigo, and Assanis, Dimitris. "A Double-Wiebe Function for Reactivity Controlled Compression Ignition Combustion Using Reformate Diesel." *Journal of Energy Resources Technology* Vol. 144 No. 22 (2022): pp.112301. DOI 10.1115/1.4053981. https://doi.org/10.1115/1.4053981.

[35] Ran, Zhongnan, Hariharan, Deivanayagam, Lawler, Benjamin, and Mamalis, Sotirios. "Experimental study of lean spark ignition combustion using gasoline, ethanol, natural gas, and syngas." *Fuel* Vol. 235 (2019): pp. 530-537. DOI 10.1016/j.fuel.2018.08.054. https://doi.org/10.1016/j.fuel.2018.08.054.

[36] Ladommatos, N. and Stone, R. "Conversion of a Diesel Engine for Gaseous Fuel Operation at High Compression Ratio." Technical Report No. SAE Technical Paper 910849. 1991. DOI 10.4271/910849. https://doi.org/10.4271/910849.

[37] Singh, S., Krishnan, S. R., Srinivasan, K. K., Midkiff, K. C., and Bell, S. R. "Effect of pilot injection timing, pilot quantity and intake charge conditions on performance and emissions for an advanced low-pilot-ignited natural gas engine." *International Journal of Engine Research* Vol. 5 No. 4 (2004): pp. 329-348. DOI 10.1243/146808704323224231. https://doi.org/10.1243/146808704323224231.

[38] Cho Muk, Haeng and He, Bang-Quan. "Spark ignition natural gas engines—A review." *Energy Conversion and Management* Vol. 48 No. 2 (2007): pp. 608-618. DOI 10.1016/j.enconman.2006.05.023. https://doi.org/10.1016/j.enconman.2006.05.023.